Jagannath University Journal of Science
Volume 11, Number I, Jun. 2024, pp. 172−185
https://jnu.ac.bd/journal/portal/archives/science.jsp
ISSN 3005-4486 (Online), ISSN 2224-1698 (Print)

Numerical Simulation of SEIR Model for COVID-19 Infection

Research Article

Hussain Muhammod Golam Rajique, Md. Asraful Islam* and Suvechchha Misty

Department of Mathematics, Jagannath University, Dhaka-1100, Bangladesh

DOI: https://doi.org/10.3329/jnujsci.v11i1.76701

Received: 1 April 2024, Accepted: 23 June 2024

ABSTRACT

One of the most basic models in epidemiology, the SEIR (Susceptible-Exposed-Infectious-Recovered) model explains how viral infections spread through communities. This study analyzes the SEIR model's differential equations to learn more about its dynamic behaviors. This study discusses the 2019 corona virus disease (COVID-19) epidemic model using numerical methods of susceptible exposed infected recovered (SEIR). A numerical description of the notion is provided using two numerical approaches, including forward Euler and RK-4 approaches. The subplots of SEIR model are drawn by ode 45 commands. The stability of disease free equilibrium and Endemic equilibrium points are depicted. The significance of comprehending the interaction between epidemiological variables and population dynamics in developing efficient public health treatments is brought to light in this study, which investigates the consequences of these equations on the transmission and management of infectious diseases. Insights into the dynamics of illness transmission and potential measures for mitigating its effects are presented through the use of mathematical analysis and computational simulations.

Keywords: *Susceptible, Transmission, Disease free equilibrium, Endemic equilibrium, Stability, Recovery rate*

1. Introduction

A vast family of viruses is known as corona viruses. All the way from the average cold to SARS and beyond, these viruses are notorious for causing a wide variety of illnesses. A major outbreak of pneumonia cases in late 2019 was shown to be caused by SARS-CoV-2. Wuhan, a city in the Chinese province of Hubei, was the site of the cluster of incidents(Chen et al. 2020). Mathematical modeling of the new corona virus is an area where numerous authors have contributed. The transmission rates of the Middle East respiratory syndrome corona virus (MERSCoV) were assessed in two separate time periods as a result of

***Corresponding Author:** Md. Asraful Islam
E-mail: asraful@math.jnu.ac.bd

significant interventions using a mathematical model for the transmission dynamics of the virus (Hsieh, 2015, Kim et al. 2016, Chen et al. 2020, Sookaromdee et al. 2020). Researchers from a wide variety of disciplines looked at the COVID-19 virus from many perspectives in an attempt to stem the spread of the disease. Pathology, sociology, infectious disease dynamics, and forecasting are all part of this framework (Zhu et al. 2020, Ji et al. 2020). COVID-19 is a novel corona virus generating a respiratory epidemic. Public health is threatened by this infectious disease's spread. This work used a modified susceptible-exposed-infectious-recovered (SEIR) compartmental mathematical model to predict COVID-19 pandemic dynamics. The environmental pathogen and medicines evaluated in this model (Samuel et al. 2020). Dengue fever, malaria, influenza, the plague, and HIV/AIDS are just a few of the diseases that have spread throughout the years. The number of outbreaks and illness transmissions has also increased significantly. The difficult but essential work of creating an appropriate epidemiological model for such epidemics must be finished. Using a network-level perspective, some researchers have attempted to model and forecast the diseases spread (Keeling et al. 2005, Prasse et al. 2020). Scientists discovered that SARS-CoV-2 exhibited a high viral load in the upper respiratory tracts of asymptomatic or mildly symptomatic individuals (Zou et al. 2020). Subclinical infection may thus be crucial to the pandemic's ability to linger. The application of mathematical models allows for the prediction and control of corona virus propagation (Anderson et al. 1992, Diekmann et al.200, Hethcote, 2000, Brauer et al. 2012). Predicting the number of cases with high accuracy is, thus, the best way to stop the pandemic from getting worse. The government can then organize their efforts to contain the pandemic more effectively. Common models that are not appropriate for epidemic impact prediction include SIR(Cantó et al. 2017, Chen et al. 2020), SEIR (Liu et al. 2004), and SEIJR (Zareie et al. 2020). This is because these models are very simplistic and fail to account for important details like asymptomatic patients, isolation instances, and other relevant elements. For this reason, it is imperative that we present a model that takes into consideration the overlooked aspects in order to acquire an accurate count of the infection cases. In a number of cases reported from India, the patient had absolutely no symptoms. Consequently, symptomless scenarios must be accounted for in the mathematical model. A new mathematical model, SEIAQRDT, was the intended outcome of this research. For this model, we expanded upon the generalized SEIR approach put out by Geng et al. (2020) and tailored it to the specific needs of India and its most hit states. Due to the continuous nature of the COVID-19 pandemic, mathematical models are helpful for monitoring the progression of the disease and predicting its future spread. In their quest to thwart such broadcasts, governments may find this data useful. There are a plethora of mathematical models being worked on right now to analyze the COVID-19 pandemic and forecast its future trajectory (Fanelli et al. 2020, Giordano et al. 2020, He et al. 2020). The number of confirmed cases of the pandemic worldwide exceeded 120 million by mid-March 2021 (Kaxiras et al. 2020). To minimize the simulation timeframes, a technique similar to that of an earlier work (Balsa et al. 2020) was used: a fixed number of independent simulations were executed for each run of the stochastic SEIR model with specific parameters to account for uncertainty. A compartmental non-autonomous diseases model is constructed by expanding upon the well-known susceptible-exposed-invectives-removed (SEIR) framework (Li, 2018, Martcheva, 2015). This indicates that, in comparison to reality, the long-term predictions are significantly inaccurate. Isolated participants are replaced with those who did not exhibit any symptoms during the SEIJR. In comparison to the SEIAR, that is the most notable difference between the two. It is utilized this model (Bai et al. 2020) in their investigation and discovered that it was similar to the SEIJR model. The model, known as SEIAQRDT throughout its development, consists of eight separate sections.

Substantially susceptible (S), exposed (E), infected (I), asymptomatic (A), quarantined (Q), recovered (R), dead (D), and inadequately susceptible (T) are all parts of these areas. In order to forecast the consequences of the pandemic, this model is applied within the framework of India and the states hit the hardest by Preety et al. (2021). Using mathematical models of epidemics is one approach (Fazal et al. 2023) to comprehend the transmission of infectious illnesses and their potential future occurrences. These findings are vital for the development of public policies that can control epidemics. The overall number of infected individuals and the duration of the epidemic are two examples of epidemic-related outcomes that can be forecasted using mathematical models. The results of various preventative interventions, such as immunization, social distance, or isolation, can also be predicted by them.

2. Formulation of SEIR model

The model consists of four compartments representing different stages of infection: susceptible individuals (S), exposed individuals (E), infectious individuals (I), and recovered individuals (R). The differential equations governing the model describe the rates of change of each compartment over time, taking into account parameters such as the transmission rate (β), the rate of transition from exposed to infectious (σ), the recovery rate (γ), and the intrinsic decease rate (μ).

$$\frac{dS}{dt} = \mu - \frac{\beta SI}{N} \quad (1)$$

$$\frac{dE}{dt} = \frac{\beta SI}{N} - \sigma E \quad (2)$$

$$\frac{dI}{dt} = \sigma(1-\alpha)E - \gamma I \quad (3)$$

$$\frac{dR}{dt} = \gamma I - \mu R \quad (4)$$

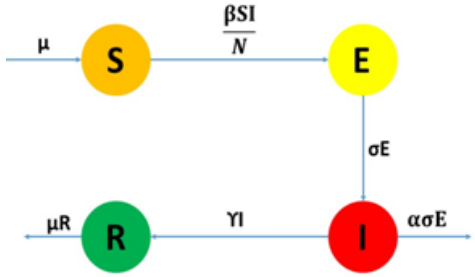

Fig. 1: Flow Chart of SEIR Model **(**1-4).

The term βSI/N is used to describe the rate of exposure for susceptible individuals. The symbol σE represents the pace at which exposed people advance to the infectious phase. The coefficient α represents the proportion of exposed individuals who never become infectious, while the equation σ(1-α)E represents the rate at which exposed individuals become contagious. The notation γI is used to represent the rate of recovery or removal of infectious persons, where γ is the rate of recovery itself. The symbol μR is used to represent the rate at which individuals depart from the restored population.

Table 1 SEIR model Description of Parameters

Parameter	Parameter Description	Parameter	Parameter Description
S	Susceptible Individuals	β	Transmission rate
E	Exposed Individuals	ϒ	Recovery rate
I	Infected Individuals	μ	Rate at which individuals enter and exit the system (births and deaths).
R	Recovered Individuals	σ	Rate at which individuals move from the exposed to the infectious compartment.
N	Total population	α	The fraction of exposed individuals who become asymptomatic.

Table 2 Initial values of parameters for S, E, I, R, β, σ, μ, α, ϒ, N

Parameter	Values	Data Source	Parameter	Values	Data Source
S	800	Assume	β	0.2	Assume
E	27	[12]	ϒ	0.05	[19]
I	100	Assume	μ	0.01	[26]
R	23	[31]	σ	0.1	Assume
N	1000	-	α	0.2	Assume

2.1 Positivity Results (Piu et al. 2020**)**

Theorem 01: *Assume the initial data set by* $(S,E,I,R)>0$, *then the solution set* $(S,E,I,R)(t)$ *of the equation (1-4) is positive for all* $t>0$.

Proof: From the equation (1) we assume

$$\frac{dS}{dt}=\mu-\frac{\beta SI}{N}=\mu-\psi_1(t)S(t)$$

Where $\psi_1(t)=\frac{\beta S(t)I(t)}{N(t)}$

By integration, we have the following expression

$$S(t)=S_0\exp\left(-\int_0^t\psi_1(t)ds\right)+\mu\exp\left(-\int_0^t\psi(s)ds\right)\int_0^t e^{\int_0^s\psi_1(u)du}ds>0$$

The above expression depicts that $S(t)$ is nonnegative for all *t*.

Similarly, E (t), I (t), and R (t) are positive for all *t*.

2.2 Existence and Uniqueness of Solution for the SEIR Model(Samuel et al. 2019)

The section that follows is a visual representation of an overall first-order ODE:

$$\xi'=h(t,\xi),\qquad \xi(t_0)=\xi_0 \tag{5}$$

$$h_1=\mu-\frac{\beta SI}{N}$$

$$h_2=\frac{\beta SI}{N}-\sigma E$$

$$h_3=\sigma(1-\alpha)E-\gamma I$$

$$h_4=\gamma I-\mu R$$

Theorem 2(Uniqueness of Solution)

Assume that the domain is represented by D

$$|t-t_0|\le a,\ \ \|\xi-\xi_0\|\le b,\ \ \xi=(\xi 1,\xi_2,\xi_3,\ldots\ldots\ldots\ldots\xi_n),\ \xi_0=(\xi_{10},\xi_{20},\xi_{30},\ldots\ldots\xi_{n0}) \tag{6}$$

And let that $h(t,\xi)$ *satisfies the Lipschitz condition:*

$$\|h(t,\xi_1)-h(t,\xi_2)\|\le M\|\xi_1-\xi_2\| \tag{7}$$

Even though there is a certain circumstance where both pairs (t,ξ_1)) and (t,ξ_2) are members of the domain D, where M is a positive constant. A distinct continuous vector solution $\xi(t)$ exists in system (5) for each non-zero constant d on the interval $|t-t_0|\le\delta$. A crucial requirement that condition (7) meets is:

$\left\{\frac{\partial h_i}{\partial\xi_j},\ i,j=1,2,\ldots n\right.$ be continuous and bounded in the domain D.

Lemma 1: *If a function* $f(t,\xi)$ *has a continuous partial derivative* $\frac{\partial h_i}{\partial\xi_j}$ *on a limited closed convex domain R, where R is a convex set of real numbers, then the function satisfies a Lipschitz condition in R.*

$$1\le\varepsilon\le R. \tag{8}$$

Finding a bounded solution of the type is hence our objective $0<R<\infty$.

Theorem 3(Uniqueness of Solution): *This domain is defined in (6) and holds in (7) and (8), therefore we'll mark it as D. An equation solution to the model system (1)-(4) is contained in domain D if that is right.*

Proof:

Let $h_1 = \mu - \frac{\beta SI}{N}$ (9)

$$h_2 = \frac{\beta SI}{N} - \sigma E \quad (10)$$

$$h_3 = \sigma(1-\alpha)E - \gamma I \quad (11)$$

$$h_4 = \gamma I - \mu R \quad (12)$$

Our proof establishes that the functions $\frac{\partial h_i}{\partial \xi_j}, i, j = 1,2,3,4$ are continuous and have boundaries. In other words, the partial derivatives are discrete as well as continuous. For all of the model equations, the following partial derivatives were examined:

From the equation (9)

$$\frac{\partial h_1}{\partial S} = -\frac{\beta I}{N}, \quad \left|\frac{\partial h_1}{\partial S}\right| = \left|-\frac{\beta I}{N}\right| < \infty$$

$$\frac{\partial h_1}{\partial E} = 0, \quad \left|\frac{\partial h_1}{\partial E}\right| = |0| < \infty$$

$$\frac{\partial h_1}{\partial I} = 0, \quad \left|\frac{\partial h_1}{\partial I}\right| = |0| < \infty$$

$$\frac{\partial h_1}{\partial R} = 0, \quad \left|\frac{\partial h_1}{\partial R}\right| = |0| < \infty$$

Similarly, from the equation (10)

$$\frac{\partial h_2}{\partial S} = \frac{\beta I}{N}, \quad \left|\frac{\partial h_2}{\partial S}\right| = \left|-\frac{\beta I}{N}\right| < \infty$$

$$\frac{\partial h_2}{\partial E} = -\sigma, \quad \left|\frac{\partial h_2}{\partial E}\right| = |-\sigma| < \infty$$

$$\frac{\partial h_2}{\partial I} = \frac{\beta I}{N}, \quad \left|\frac{\partial h_2}{\partial I}\right| = \left|\frac{\beta I}{N}\right| < \infty$$

$$\frac{\partial h_2}{\partial R} = 0, \quad \left|\frac{\partial h_2}{\partial R}\right| = |0| < \infty$$

From the equation (11)

$$\frac{\partial h_3}{\partial S} = 0, \quad \left|\frac{\partial h_3}{\partial S}\right| = |0| < \infty$$

$$\frac{\partial h_3}{\partial E} = \sigma(1-\alpha), \quad \left|\frac{\partial h_3}{\partial E}\right| = |\sigma(1-\alpha)| < \infty$$

$$\frac{\partial h_3}{\partial I} = -\gamma, \quad \left|\frac{\partial h_3}{\partial I}\right| = |-\gamma| < \infty$$

$$\frac{\partial h_3}{\partial R} = 0, \quad \left|\frac{\partial h_3}{\partial S}\right| = |0| < \infty$$

From the equation (12)

$$\frac{\partial h_4}{\partial S} = 0, \quad \left|\frac{\partial h_4}{\partial S}\right| = |0| < \infty$$

$$\frac{\partial h_4}{\partial E} = 0, \quad \left|\frac{\partial h_4}{\partial E}\right| = |0| < \infty$$

$$\frac{\partial h_4}{\partial I} = \gamma, \quad \left|\frac{\partial h_4}{\partial I}\right| = |\gamma| < \infty$$

$$\frac{\partial h_4}{\partial R} = 0, \quad \left|\frac{\partial h_4}{\partial R}\right| = |0| < \infty$$

It is without dispute that these partial derivatives are continuous and bounded; hence, we can assert that the D-region includes a singular solution to the (1)-(4) equations, in accordance with Theorem (2).

3. Stability Analysis

The system (1-4) has a Disease-Free Equilibrium (DFE) point for the given SEIR model is $(\boldsymbol{S_0}, \boldsymbol{E_0}, \boldsymbol{I_0}, \boldsymbol{R_0}) = \left(\frac{\mu N}{\beta}, \mathbf{0}, \mathbf{0}, \mathbf{0}\right)$*and an endemic equilibrium*

$points(\boldsymbol{S}^*, \boldsymbol{E}^*, \boldsymbol{I}^*, \boldsymbol{R}^*)=\left(\frac{\mu N}{\beta}, \frac{\mu}{\sigma}, \frac{\mu(1-\alpha)}{\gamma}, (1-\alpha)\right)$ *respectively.*

The Jacobean of the system (1-4) is

$$J=\begin{pmatrix} -\beta I/N & 0 & -\beta S/N & 0 \\ \beta I/N & -\sigma & \beta S/N & 0 \\ 0 & \sigma(1-\alpha) & -\gamma & 0 \\ 0 & 0 & \gamma & -\mu \end{pmatrix}$$

3.1 Stability at Disease Free Equilibrium Point

Jacobean matrix at the DFE point is,

$$J_{DFE}=\begin{pmatrix} -\beta I_0/N & 0 & -\beta S_0/N & 0 \\ \beta I_0/N & -\sigma & \beta S_0/N & 0 \\ 0 & \sigma(1-\alpha) & -\gamma & 0 \\ 0 & 0 & \gamma & -\mu \end{pmatrix}$$

Suppose I_0=1 and by using MATLAB we find that, the eigenvalues are $-\frac{\beta}{N}, -\sigma, -\gamma, -\mu$. The Disease-Free Equilibrium (DFE) point is asymptomatic stable.

3.2 Stability at Endemic Equilibrium Point

Jacobean matrix at the EE point is,

$$J_{EE}=\begin{pmatrix} -\beta \frac{I^*}{N} & 0 & -\beta \frac{S^*}{N} & 0 \\ \beta \frac{I^*}{N} & -\sigma & \beta \frac{S^*}{N} & 0 \\ 0 & \sigma(1-\alpha) & -\gamma & 0 \\ 0 & 0 & \gamma & -\mu \end{pmatrix}$$

Now, substitute $\boldsymbol{S}^*, \boldsymbol{E}^*, \boldsymbol{I}^*, \boldsymbol{R}^*$

$$J_{EE}=\begin{pmatrix} -\beta\mu(1-\alpha)/N\gamma & 0 & -\mu & 0 \\ \beta\mu(1-\alpha)/N\gamma & -\sigma & \mu & 0 \\ 0 & \sigma(1-\alpha) & -\gamma & 0 \\ 0 & 0 & \gamma & -\mu \end{pmatrix}$$

The MATLAB database was used to generate a visualization that shows the biggest eigenvalues of the formula J(E*). Based on the previous image, it is evident that the maximum value of the Jacobean spectral radius is smaller than one, proving the correctness of the assumed assertion [31]. By using MATLAB we find that, the eigenvalues are $-\frac{\beta\mu(1-\alpha)}{N\gamma}, -\sigma, -\gamma, -\mu$. The Endemic Equilibrium (EE) point is asymptomatic stable.

4. Numerical Simulations of Dynamical Behavior

The findings are discussed in detail in this section. Additionally, Euler and RK-4 methods in the model are compared in terms of their use.

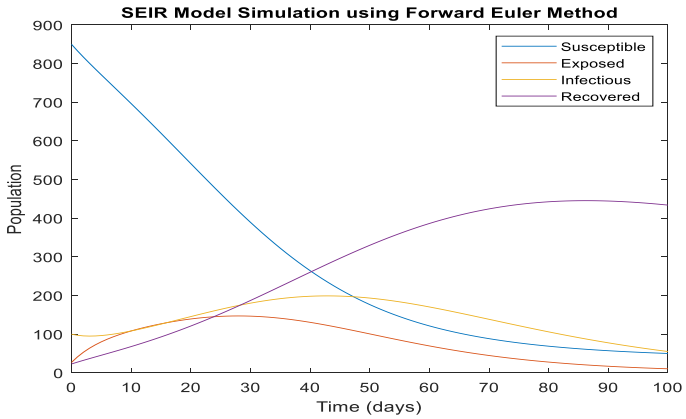

Fig. 2: Dynamics of SEIR model (1-4) by using Euler Method; initial value (N=1000, S=800, E=10, I=100, R=23, β=0.2, σ=0.1, α=0.2, μ=0.01 and ϒ=0.05, h=1).

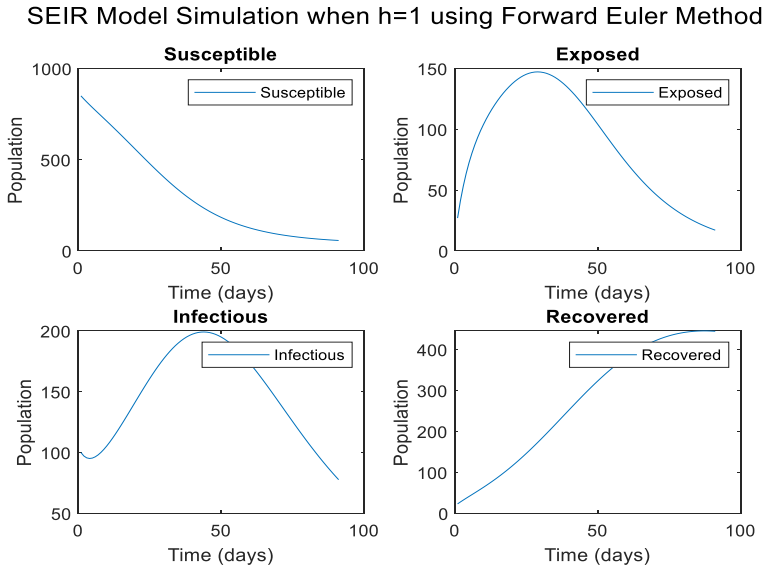

Fig.3: Dynamics of SEIR model (1-4) by using Euler Method; initial value (N=1000, S=800, E=10, I=100, R=23, β=0.2, σ=0.1,α=0.2, μ=0.01 and ϒ=0.05, h=1).

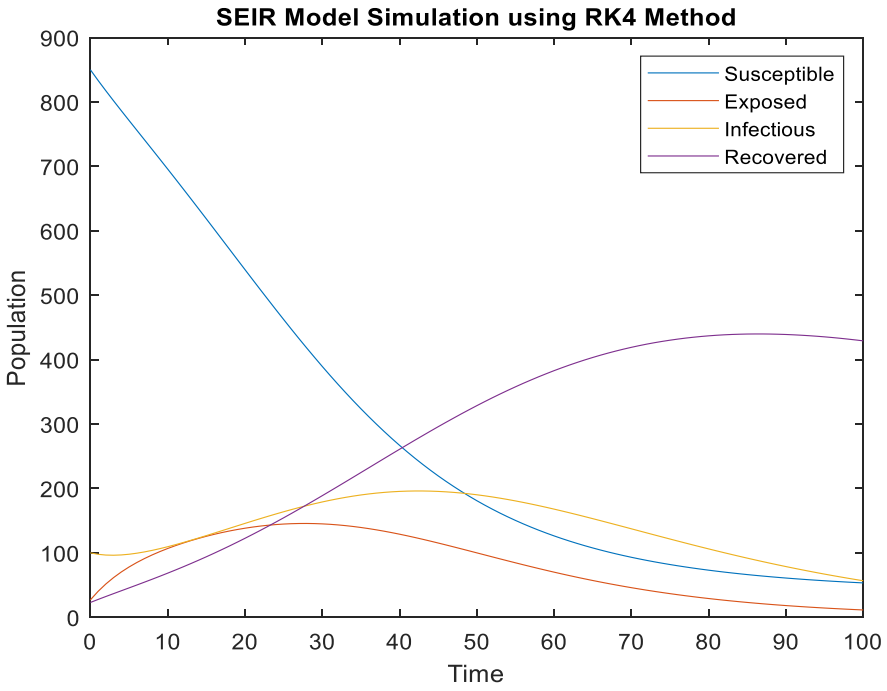

Fig.4: Dynamics of SEIR model (1-4) by using RK-4; initial value (N=1000, S_0=800, E=10, I=100, R=23, β=0.2, σ=0.1, α=0.2, μ=0.01,ϒ=0.05 and h=1).

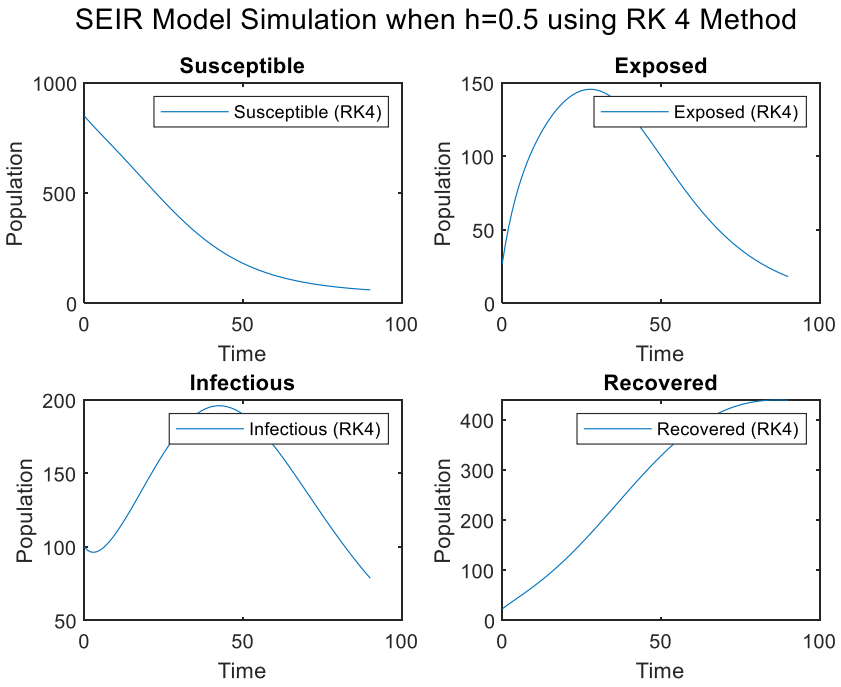

Fig.5: Dynamics of SEIR model (1) by using RK-4; initial value (N=1000, S_0=800, E=10, I=100, R=23, β=0.2, σ=0.1,α=0.2, μ=0.01,ϒ=0.05 and h=1).

The SEIR model's behavior is depicted in the graphs up above. Figures 5 and 6 show how the Euler technique behaves favorably for minor step sizes h=1. Figures 7 and 8, which implement the RK-4 approach, demonstrate that the model exhibits identical characteristics at step sizes h=1.

S-Susceptible:

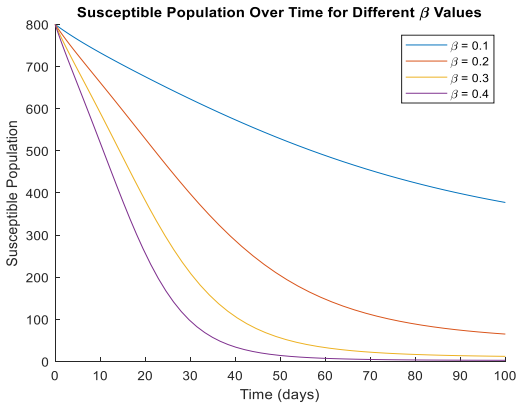

(a)

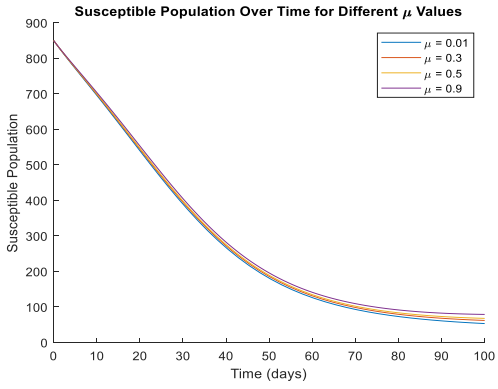

(b)

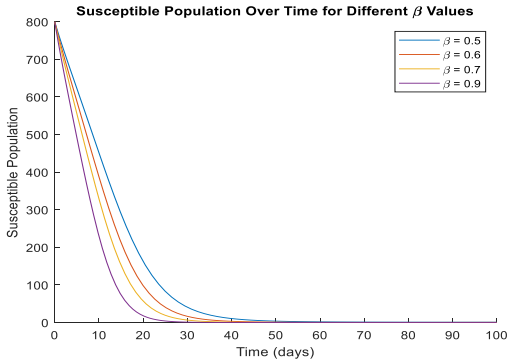

(c)

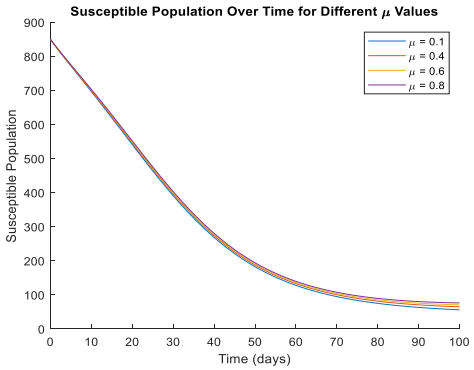

(d)

Fig. 6: Dynamics of Susceptible individual (S):(a), (b), (c), and (d) with initial value (N=1000, S=800, σ=0.1, α=0.2, $\Upsilon = \mathbf{0.05}$).

The behavior of the susceptible population (S) equation graph in the SEIR model for different values of β and μ depends on how these parameters influence the dynamics of disease transmission and population growth.

Here's an overview of the expected behaviors:A higher transmission rate leads to a faster spread of the disease within the population. This results in a more rapid decrease in the susceptible population over time because more individuals are becoming infected at a faster rate.Conversely, a lower transmission rate slows down the spread of the disease, resulting in a slower decrease in the susceptible population over time.A higher birth rate increases the rate at which new susceptible individuals enter the population. This tends to counteract the decrease in the susceptible population due to disease transmission, resulting in a slower decline or even an increase in the susceptible population over time.Decreasing μ: Conversely, a lower birth rate reduces the influx of new susceptible individuals into the population, which may accelerate the decrease in the susceptible population over time.

E-Exposed:

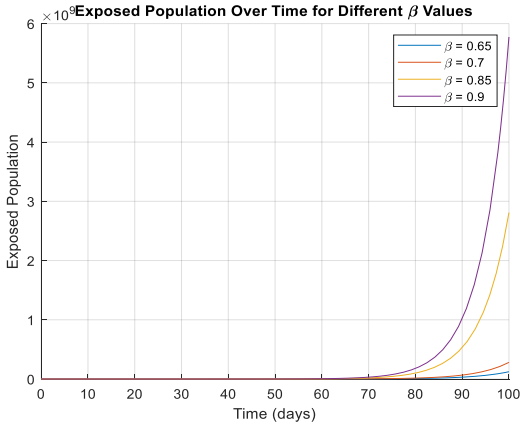

(e)

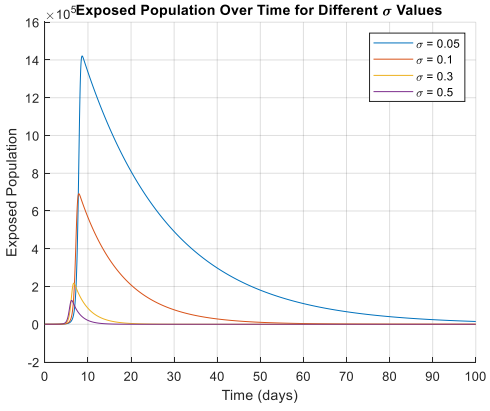

(f)

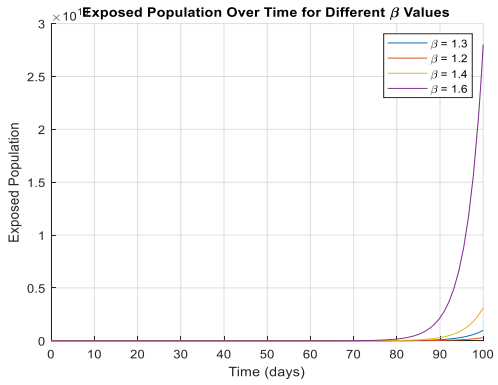

(g)

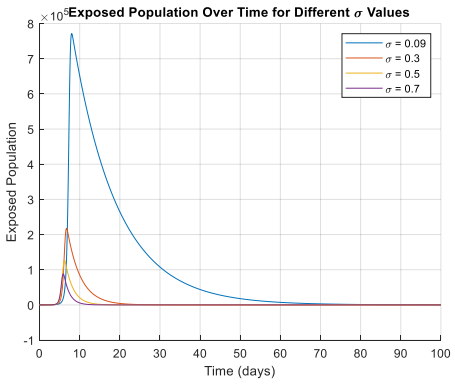

(h)

Fig. 7: Dynamics of Exposed Individuals (E): (e), (f), (g), and (h) with initial value (E=10).

Higher transmission rates lead to more swiftpropagation of the disease within the population. This can result in a steeper increase in the exposed population early in the outbreak, as more susceptible individuals become exposed to infectious individuals at a faster rate.Lower transmission rates slow down the spread of the disease, resulting in a slower increase in the exposed population over time.Increasing σ: A higher rate of transition from the exposed to the infectious state means that individuals spend less time in the latent period. This can lead to a time frame of implantation that is shorter and a quicker rise in the infectious population, potentially resulting in a sharper peak in the exposed population before it declines. Conversely, a lower rate of transition results in a longer latent period, leading to a more gradual increase in the exposed population and potentially a smoother curve overall.When observing the graph of the exposed population over time for different values of σ and β, we may notice the following patterns:

- Higher values of both β and σ generally lead to more rapid increases in the exposed population and earlier peaks.
- Lower values of β and σ result in slower increases and delays in the peak of the exposed population.
- The specific shape and timing of the curve will depend on the interplay between these parameters and other factors such as population size, initial conditions, and the effectiveness of control measures.

I-Infected:

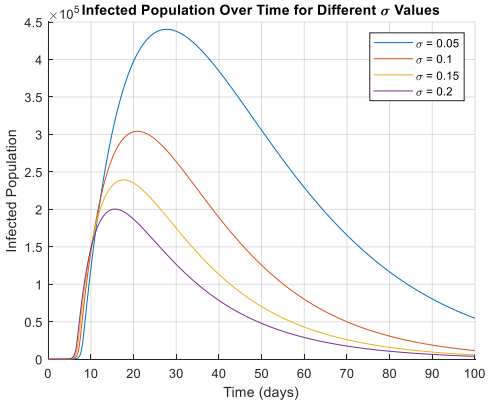

(i)

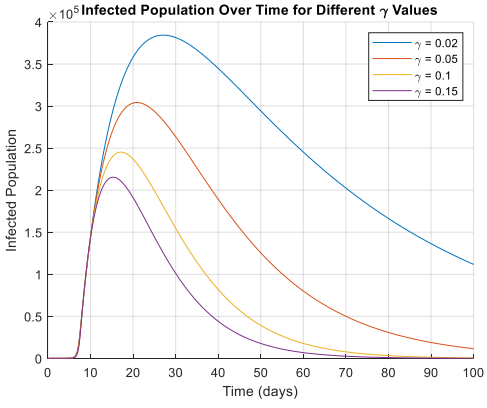

(j)

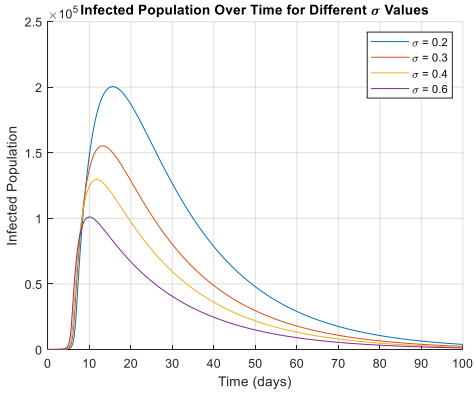

(k)

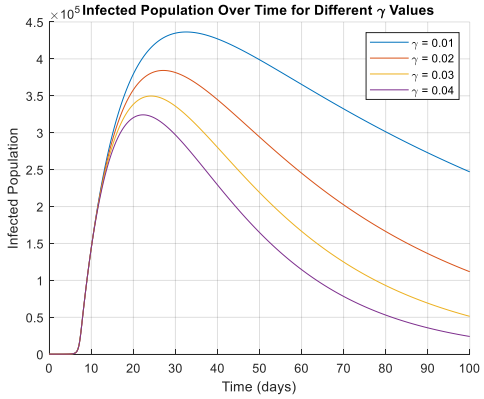

(l)

Fig. 8: Dynamics of Infected (I): (i), (j), (k), and (l) with initial value (E=27, I=100).

Increasing the transmission rate (σ) typically results in a faster spread of the disease, leading to a higher peak in the infectious population. This is because a higher transmission rate means that exposed individuals become infectious more quickly.Decreasing the transmission rate slows down the spread of the disease, resulting in a lower peak in the infectious population. This occurs because exposed individuals take longer to become infectious.Increasing the recovery rate (γ) speeds up the recovery process, causing infectious individuals to recover and leave the infectious compartment more quickly. This results in a shorter duration of the epidemic and a lower peak in the infectious population.Decreasing the recovery rate slows down the recovery process, prolonging the duration of the epidemic and leading to a higher peak in the infectious population.The dynamics of the infectious population are influenced by the interplay between σ and γ. Higher values of σ accelerate the spread of the disease, while higher values of γ accelerate recovery. The combination of these parameters determines the overall trajectory of the epidemic, including the peak height, duration, and eventual decline of the infectious population.Depending on the specific values of σ and γ, the infectious population may exhibit stable behavior, where it reaches a peak and then declines steadily. In some cases, particularly when the parameters are finely balanced, oscillations or fluctuations in the infectious population may occur over time.

R-Recovered:

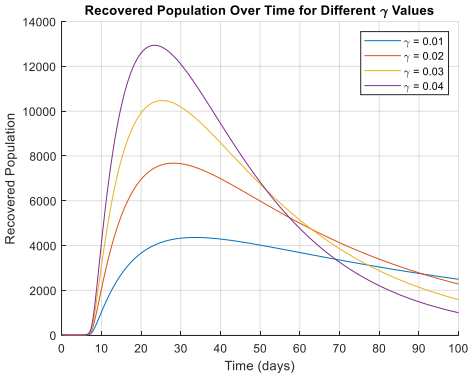

(m)

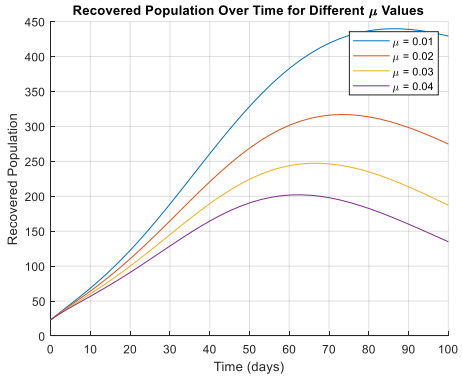

(n)

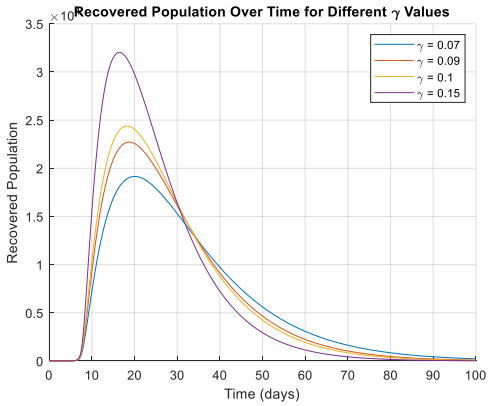

(o)

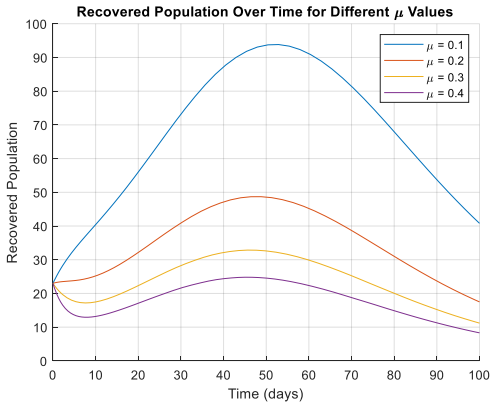

(p)

Fig. 9: Dynamics of Recovered (R): (m), (n), (o), and (p) withinitial value (I=100).

Higher values of γ lead to faster recovery rates. As a result, the duration of the epidemic curve shortens, and the peak of the infectious population decreases. Lower values of γ prolong the duration of the epidemic curve and increase the peak of the infectious population. μ affects the total population size over time due to natural mortality. If μ is significant, it can reduce the overall population size, affecting the dynamics of the disease spread.However, in most SEIR models, μ is relatively small compared to other rates such as transmission and recovery rates. Therefore, its effect on the dynamics may be less pronounced compared to other parameters.The interplay between γ and μ can influence the overall impact of the disease on the population. Higher γ values may counteract the effect of μ by reducing the duration of infectiousness, thereby limiting the number of deaths due to the disease.

Conversely, if μ is relatively high and γ is low, the disease may have a more significant impact on mortality, especially in scenarios where healthcare resources are limited.

5. Conclusion

When examining the susceptible equation graph, the parameters' implications on population management and disease control are examined. Graph shape would also be influenced by additional model parameters, initial conditions, and outside variables influencing the dynamics of the population and the spread of illness. The behavior of the infectious population graph over time is influenced by the parameters σ, γ, and their interplay. Predicting and limiting infectious disease spread requires understanding how these characteristics affect epidemic dynamics. The infectious population graph's behavior over time depends on the interaction between γ and μ, which impact disease propagation and population dynamics. High γ values promote faster recovery and lower infectious peaks, while high μ values may affect population growth and mortality rates. The SEIR model has shown the complicated relationship between epidemiological factors and population dynamics in COVID-19 transmission dynamics. Our research of SEIR equations reveals how characteristics like transmission rate (β),rate of transition from exposed to infectious (σ), recovery rate (γ), and birth rate (μ) impact disease spread and control in populations. Our data show that public health initiatives are crucial to COVID-19

mitigation. Effective strategies include social distancing, mask-wearing, vaccination campaigns, and quarantine have reduced transmission rates (β) and slowed the epidemic curve. Our analysis highlights the significance of including population dynamics (μ) alongside illness characteristics, as demographic considerations can considerably impact control methods' effectiveness. Our analysis emphasizes the need for ongoing COVID-19 surveillance and policy adaptation. As novel variations emerge and vaccination efforts evolve, tactics must be reassessed and refined to manage transmission dynamics while minimizing social and economic disturbances. Future studies may use more complex models that combine regional heterogeneity, age structure, and behavioral dynamics to better explain COVID-19 transmission dynamics and inform targeted treatments. The findings underscore the importance of timely intervention strategies, such as social distancing, mask mandates, and vaccination campaigns, in mitigating the spread of COVID-19. The SEIR model can inform decision-making by predicting the impact of different interventions on disease transmission dynamics. Our research expands COVID-19 epidemiological expertise and emphasizes the need for interdisciplinary approaches to global health issues. Mathematical modeling and empirical data help us understand infectious disease dynamics and develop sustainable control and prevention techniques.

References

Anderson RM, May RM. 1992. Infectious diseases of humans: dynamics and control. Oxford University Press Inc., New York.

Brauer F, Chavez CC. 2012. Mathematical models in population biology and epidemiology. Springer, New York, NY.

Balsa C, Lopes I, Rufino J, Guarda T. 2020. An exploratory study on the simulation of stochastic epidemic models, *Advance in intelligent Systems and computing*, 71159: 26–736.

Bai Y, Liu K, Chen Z. 2020. Early transmission dynamics of novel coronavirus pneumonia epidemic in Shaanxi Province, *Chinese Journal of Nosoconmiology*, 30(6):834–838.

Chen N, Zhou M, Dong X, Qu J, Gong F, Han Y, Qiu Y, Wang J, Liu Y, WeiY, et al. 2020. "Epidemiological and clinical characteristics of 99 cases of 2019novel coronavirus pneumonia in Wuhan, China: a descriptive study", *Lancet*, 395: 507–13.

Chen TM, Rui J, Wang QP, Zhao ZY, Cui JA, Yin L. 2020. A mathematical model for simulating the phase-based transmissibility of a novel coronavirus. *Infectious Diseases Proverty*, 9(1): 1-8.

Cantó B, Coll C, Sánchez E. 2017. Estimation of parameters in a structured SIR model, *Advance Differential Equations*, 33(1):16-27.

Chen Y, Cheng J, Jiang Y, Liu K. 2020. A time delay dynamical model for outbreak of 2019-nCoV and the parameter identification. *Journal of Inverse III-Posed Problems* 28(2): 243–250.

Diekmann O, Heesterbeek JAP. 2000. Mathematical epidemiology of infectious diseases: model building, analysis and interpretation, John Wiley and Sons, Chichester.

Fanelli D, Piazza F. 2020. Analysis and forecast of COVID-19 spreading in China,Italy and France. *Chaos Solitons Fractals*, 134: 109-120.

Fazal D, Muhammad I. 2023. Construction and Analysis of a Nonstandard Computational Method
for the Solution of SEIR Epidemic Model, *Scientific Inquiry and Review*, 7(1): 87-110.

Geng H, Xu A, Wang X, Zhang Y, Yin X, Mao MA. 2020. Analysis of the role of current prevention and control measures in the epidemic of new corona virus based on SEIR model, Journal of Jinan University 41(2): 1–7.

Giordano G, et al. 2020. Modeling the COVID-19 epidemic and implementation of population-wide interventions in Italy, *Nature Medicine*. 26: 855–860.

Hsieh YH. 2015. "Middle East respiratory syndrome coronavirus (MERSCoV) nosocomial outbreak in South Korea: insights from modeling". *PeerJournal*, 3:1505.

He S, Peng Y, Sun K. 2020. SEIR modeling of the COVID-19 and its dynamics, *Nonlinear Dynamics*, 101: 1667–1680.

Hethcote H. 2000. The mathematics of infectious diseases. *SIAM Review*, 42(4): 599–653.

Ji, W, Wang, W, Zhao, X, et al. 2020. Cross-species transmission of the newly identified corona virus 2019-ncov. Journal of Medical Virology. 92: 433–440.

Kim Y, Lee S, Chu C, Choe S, Hong S, Shin Y. 2016. "The characteristics of middleeastern respiratory syndrome coronavirus transmission dynamics inSouth Korea" *Osong Public Health Res Perspect*. 7(1): 49–55.

Kaxiras E, Neofotistos G, Angelaki E. 2020. The first 100 days: modeling the evolution of the COVID-19 pandemic, *Chaos Solitons Fractals*, 138: 110-121.

Keeling MJ, Eames KTD. 2005. Networks and epidemic models, *Journal of the Royal Society Interface* 2: 295–307.

Liu C, Ding G, Gong J, Wang L, Cheng K, Zhang D. 2004. Studies on mathematical models for SARS outbreak prediction and warning. *Chinese Science Bulletin*, 49(21): 2245–2251.

Li MY. 2018. An introduction to mathematical modeling of infectious diseases. Springer, New York.

Martcheva M. 2015. An introduction to mathematical epidemiology, Springer, New York.

Prasse B, Achterberg MA, Ma L. et al. 2020. Network-based prediction of the 2019-ncov epidemic outbreak in the chineseprovince hubei, Applied Network Science, 5(1): 1-11.

Preety K, Harendra PS, Swarn S. 2021. SEIAQRDT model for the spread of novel corona virus (COVID-19): A case study in India, Journal *of Applied Intelligence*, 51:2818–2837.

Piu S., Jayanta M., Subhas K. 2020. A mathematical model for COVID-19 transmission dynamics with a case study of India, Chaos, Solitons and Fractals, 140: 110173.

Sookaromdee P, Wiwanitkit V, et al. 2020. Imported cases of 2019-novel coronavirus (2019-ncov) infections in Thailand: mathematical modelling of theoutbreak. *Asian Pacific Journal Tropical Medicine*, 13(3):139–40.

Samuel M, Mark K, Viona O, Duncan, Rachel M. 2020. SEIR model for COVID-19 dynamics incorporating the environment and social distancing, *BMC research notes*, 13: 2-5.

Samuel OS, Daouda S, Abdullahi AI, Isaac AP. 2019. On the Existence, Uniqueness, Stability of Solution and Numerical Simulations of a Mathematical Model for Measles Disease, International Journal of Advances in Mathematics, 2019: 84-111.

Zhu N, Zhang D, Wang D. 2020. A novel corona virus from patients with pneumonia in china, 2019, *New England Journal of Medicine*, 382: 727-733.

Zou L, Ruan F, Huang M, Liang L, Huang H, Hong Z, Yu J, Kang M, Song Y, Xia J, Guo Q, Song T, He J, Yen HL, Peiris M, Wu J. 2020. SARS-CoV-2 viral load in upper respiratory specimens of infected patients. *New England Journal of Medicine*, 382(12):1177–1179.

Zareie B, Roshani A, Mansournia MA, Rasouli MA, Moradi G. 2020. A model for COVID-19 prediction in Iran based on China parameters, *Journal of Archieves Iranian Medicine*, 23(4): 244–248.